Engineering Journal issn: 0125-8281

Article

Quality Improvement of Low-Grade Calcium Carbonate Using Induced Roll Magnetic Separator

Pimpichcha Teawpanich[1], Somsak Saisinchai[1], Apisit Numprasanthai[1], Raphael Bissen[1], Onchanok Juntarasakul[1], Carlito Baltazar Tabelin[2], and Theerayut Phengsaart[1,*]

1 Department of Mining and Petroleum Engineering, Faculty of Engineering, Chulalongkorn University, Bangkok 10330, Thailand
2 Department of Materials and Resources Engineering Technology, College of Engineering, Mindanao State University - Iligan Institute of Technology, Iligan City 9200, Philippines
*E-mail: theerayut.p@chula.ac.th (Corresponding author)

Abstract. Calcium carbonate ($CaCO_3$) is an essential raw material in the manufacture of goods and industrial products like cement, rubber, paper, paints, food, and medicines. For this compound to be economically valuable, however, its quality needs to meet the standard market requirements. Among the various impurities found in natural $CaCO_3$-bearing ores, iron (Fe) is one of the most problematic. In this study, the upgrading of low-grade $CaCO_3$ from a processing plant in Thailand by magnetic separation was investigated. Detailed characterization of the low-grade material was also carried out to identify the solid-phase partitioning of Fe. The results showed that Fe was mainly associated with magnetite and pyrrhotite in the ore, and during processing, additional Fe was introduced from the ball milling process. To improve the quality of this low-grade $CaCO_3$, the effects of magnetic field intensity, feed rate, and repetition on the induce roll magnetic separation were investigated. Based on the results, higher magnetic field intensity, lower feed rate, and more repetition are required for the upgrading of low-grade $CaCO_3$.

Keywords: Calcium carbonate, limestone, magnetic separation, iron content, ball mill.

ENGINEERING JOURNAL Volume 27 Issue 10
Received 1 April 2023
Accepted 25 September 2023
Published 31 October 2023
Online at https://engj.org/
DOI:10.4186/ej.2023.27.10.1

DOI:10.4186/ej.2023.27.10.1

1. Introduction

Calcium carbonate ($CaCO_3$) is usually found as the mineral calcite [1–3]. Calcite is a major mineral component of sedimentary rocks like chalk, limestone, sandstones, and mudstones [4–6] which are typically formed by the deposition of shells from snails, shellfish, and coral in ancient fresh and marine environments [7].

Calcium carbonate is used as raw material in cement, plastic, paint, paper, and pharmaceutical manufacturing industries. In general, pure calcite is transparent and colorless but rarely found in nature. In contrast, there are various colors of calcite that could be found due to the impurity of metal ions (i.e., Fe, Zn, Co, and Mn) replace calcium ions in the crystal lattice [1]. Table 1 summarizes the typical specifications of $CaCO_3$ by industries in Thailand. To obtain the products with acceptable properties, the quality of raw materials needs to be controlled following market and/or industrial standards. For $CaCO_3$-bearing raw materials, higher prices are given to those with finer particle size is finer, higher $CaCO_3$ content, lower impurities especially Fe, and less discoloration (high whiteness).

To prepare a product that meets the standard requirements for animal feeds and fillers for rubber, paper, paint, coating, and pharmaceutical products, the Fe (as Fe_2O_3) content must be less than 0.1 and 0.05%, respectively. Therefore, $CaCO_3$ with trace Fe impurities (>0.1% as Fe_2O_3) is difficult to use since the impurities could decrease the whiteness and durability of products [8].

Although $CaCO_3$ is ubiquitous, high-grade deposits are only available in few locations. In Thailand, premium-grade $CaCO_3$ is produced from the Khoktum deposit, Lopburi Province. High-grade $CaCO_3$ is mined, processed, and utilized by various industries, but because it is a non-renewable resource, such deposits are gone forever once depleted. Because the majority of available high-grade deposits have been used up in the past, those that are available today for exploitation are typically of lower grade.

The lack of raw materials for various applications due to the limited availability of mineral resources is becoming a serious issue in recent times. For these resources to be enough for our generation as well as to preserve them for the future, they should be used properly by following the United Nations' Sustainable Development Goals (UN-SDGs) especially, Goal 12 "Responsible Consumption and Production" [9–12].

To achieve this goal, technologies to improve the quality of low-grade mineral resources need to be developed. For $CaCO_3$, the main impurity that must be controlled is the Fe content of the product after mining and processing. Unfortunately, products generated from low-grade $CaCO_3$ showed a higher content of Fe_2O_3 than the standard requirement. For Fe-rich $CaCO_3$ deposits, magnetic separation is a potentially promising approach for the removal of Fe-bearing minerals because the majority of them have high magnetic susceptibilities; that is, they are easily removed using a strong magnetic field [13–15].

Magnetic separation is a technique widely used in mineral processing as well as resources recycling. Minerals can be categorized into three types based on their magnetic properties: ferromagnetic, paramagnetic, and diamagnetic. For ferromagnetic minerals, they are easily recovered and separated from diamagnetic minerals using permanent magnets with low magnetic intensities. In contrast, paramagnetic minerals are more difficult to recover and separate, so high magnetic intensity is required [16–39].

Induced roll magnetic separator (IRMS) is a simple and robust dry-type magnetic separator well-known for its high efficiency in separating paramagnetic materials from ores. It is widely used for the separation of hematite, ilmenite, wolframite, cassiterite, phosphate rocks, glass sands, and beach sands [40–44]. The IRMS consists of a revolving phosphate steel laminated roll that is compressed with a non-magnetic stainless-steel shaft. The rotor is placed between specially shaped poles of an electromagnet. The two different roll laminations together with the shaft with a serrated profile could promote high magnetic intensities of up to 2.2 T. During separation, magnetic particles are attracted by the magnetic roll and are recovered into the magnetic compartment while the non-magnetic particles are thrown off into another roll or non-magnetic compartment.

Table 1. Typical specifications of calcium carbonate for industries in Thailand.

Specification	Industries				
	Animal feeds	**Rubber**	**Paper**	**Paint & coating**	**Pharmaceuticals**
Particle size [μm]	< 100 μm	< 50 μm (100%) & with < 2 μm (50 %)			
$CaCO_3$ [%]	>98		> 98.5		
Fe_2O_3 [%]	≤0.1	0.03–0.05	0.02–0.03	0.01–0.02	< 0.01
Whiteness [%]	>94		>95		
Price [USD]	17–22	22–28	28–55	70–140	140–225

The important parameters affecting the separation efficiency of IRMS include magnetic susceptibility of particles, particle size, applied magnetic field intensity, feed rate, roller speed and angle of product collection splitter [42, 44]. The application of IRMS for the removal of Fe-bearing materials from $CaCO_3$ should be evaluated and explored. The application of this separator for improvement of the separation efficiency in existing processing circuits will also increase if a better understanding of knowledge gaps is achieved [44].

In this study, the chemical composition of low-grade $CaCO_3$ obtained from this processing plant was analyzed to find the source of the high Fe content. Magnetic separation experiments using a dry-type induced roll magnetic separator were carried out to improve the quality of $CaCO_3$ products by removing Fe-bearing materials to meet market requirements.

2. Materials and methods

2.1. Sample Collection and Characterization

The samples used in this study were collected from a $CaCO_3$ processing plant in Thailand. Figure 1 shows the schematic flowchart while the collection points are explained in Table 2. Low-grade $CaCO_3$ from mining with particle size less than 6 inches (≈ 150 mm) are fed into the hoppers, then screened by a 2-inch (≈ 50 mm) aperture grizzly feeder. The 2–6 inches fraction is fed into a jaw crusher to reduce the particle size to less than 2 inches. Products from the jaw crusher and particles less than 2 inches from grizzly feeder are both fed into an impact crusher with 10 mm screen, and the resulting undersize is sent to silos. At this stage, Fe-bearing

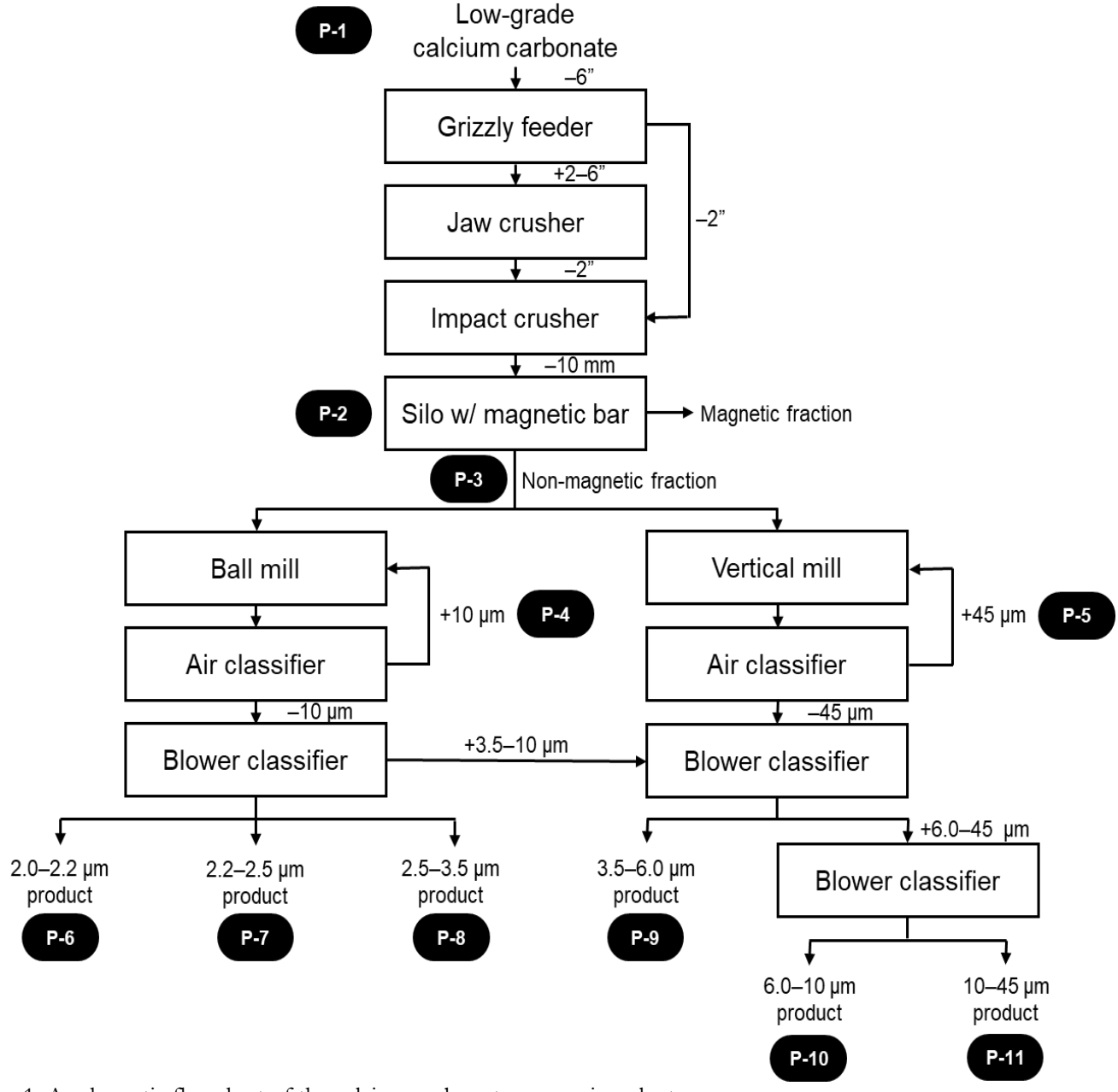

Fig. 1. A schematic flowchart of the calcium carbonate processing plant.

Table 2. The $CaCO_3$ and Fe_2O_3 contents of samples at each collection point are shown in Fig. 1.

Sample ID	Collecting points	$CaCO_3$ [%]	Fe_2O_3 [%]
P-1	Feed of low-grade $CaCO_3$	98.19	0.46
P-2	Stock in silo	98.19	0.46
P-3	Non-magnetic fraction from silo	99.09	0.05
P-4	Underflow of air classifier after ball mill	98.06	0.67
P-5	Underflow of air classifier after vertical mill	99.16	0.06
P-6	2.0–2.2 μm product	99.06	0.07
P-7	2.2–2.5 μm product	99.20	0.04
P-8	2.5–3.5 μm product	99.10	0.05
P-9	3.5–6.0 μm product	99.10	0.04
P-10	6.0–10 μm product	99.12	0.05
P-11	10–45 μm product	98.97	0.06

components, which are mostly large steel particles, are removed using permanent magnetic bars installed at the product-end of the silos. From the silos, non-magnetic products are fed into two parallel lines of the grinding process: (i) ball mill, and (ii) vertical mill.

For the ball mill line, the non-magnetic product from the crushing circuits is ground and sized using an air classifier. The >10 μm is re-ground while the <10 μm fraction is classified into final products with various sizes (i.e., 2.0–2.2, 2.2–2.5, and 2.5–3.5 μm) using a blower classifier while the 3.5–10 μm size fraction is sent to the primary blower classifier of the vertical milling line. For the vertical mill line, the non-magnetic product is ground and then classified using an air classifier. The >45 μm fraction is re-ground while the <45 μm fraction is classified into final products with various sizes (i.e., 3.5–6.0, 6.0–10, and 10–45 μm) using blower classifiers.

The chemical and mineralogical compositions of samples was analyzed using an X-ray fluorescence (XRF) spectrometer (Supermini 200, Rigaku Corporation, Japan) and X-ray diffractometer (XRD, PANalytical Aeris model, The Netherlands).

2.2. Magnetic Separation Experiments

To improve the quality of low-grade $CaCO_3$ materials, the samples with the highest Fe content were tested with magnetic separation experiments using a bench-scale IRMS (CP887412 model, Eriez Magnetics Japan Co., Ltd. Tokyo Japan) (Fig. 2), which has an induced roll width of 13.5 cm and an electrical voltage of 100 V. 1 kg of sample was used, and three magnetic field intensities—0.25, 0.35, and 0.45 T—and three feed rates—2.4, 2.8, and 3.2 kg/h—were evaluated. After the experiments, the non-magnetic fractions were weighed and analyzed by XRF.

3. Results and Discussion

3.1. Quantitative Analysis Using X-ray Fluorescence Spectroscopy

Table 2 shows the $CaCO_3$ and Fe_2O_3 contents in the samples. The high-grade $CaCO_3$ of this mine usually contains 99.2% $CaCO_3$ and 0.03% Fe_2O_3. However, the low-grade $CaCO_3$ (P-1) from mining contains 98.2% $CaCO_3$ and 0.46 % Fe_2O_3, indicating that the lower quality of the feed was inherent of the source rock. The quality remained the same after screening using the grizzly feeder and crushing with jaw and impact crushers (P-2). After the removal of magnetic fractions with a permanent magnet at the product-end of silo (P-3), the quality was improved; that is, the $CaCO_3$ content increased to 99.1% while the Fe_2O_3 content decreased to 0.05%. This product quality is good enough to be sold as fillers to the rubber manufacturing industries (Table 1).

Unfortunately, the Fe_2O_3 content increases after the grinding processes, especially using a ball mill while only a small increment was found when using a vertical mill. As shown in Table 2, Fe_2O_3 content of the air classifier underflow fraction after ball milling (P-4) was 0.67%, which was higher than the source rock (P-1; 0.46% Fe_2O_3). This indicates that the increase in Fe_2O_3 likely originated from abrasion of steel balls with each other and the liners of the ball mill. Because of this, the highest Fe_2O_3 content was measured at 0.07% in the P-6 sample, which is the finest product (2.0–2.2 μm). To confirm that Fe originated from both the source rock and ball milling, the P-3 and P-4 samples were analyzed using XRD.

3.2. Qualitative Analysis Using X-ray Diffraction

To confirm the source of Fe, the P-3 and P-4 samples were analyzed by XRD. Unfortunately, the peaks of minor materials were very weak due to the high concentration of $CaCO_3$. To detect these impurities, especially the Fe-bearing materials, magnetic separation was carried out prior to XRD. This preconcentration step was carried out using 1 kg of samples and was treated using IRMS with magnetic field intensity and feed rate of 0.45 T and 2.4 kg/h, respectively.

For P-3 sample, the results showed that Fe was mainly in the form of magnetite and pyrrhotite that came from the source rock. Magnetite is generally found in many kinds of rock, especially in the contact zones with metamorphic and country rocks. In the case of pyrrhotite,

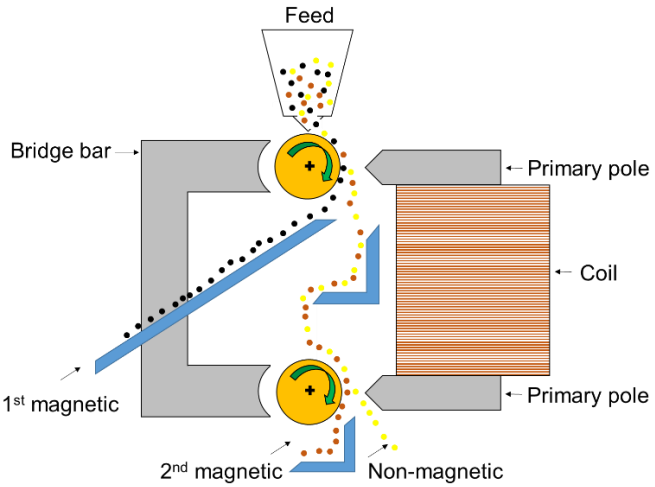

Fig. 2. A schematic illustration of the induced roll magnetic separator used in this study.

it is a common trace constituent of mafic igneous rocks and could also be found in the contact zones between the metamorphic and country rocks, together with other Fe-bearing minerals like magnetite and pyrite [45–47]. In the mining area where the samples of this study were collected, greyish-white calcite was formed by the re-crystallization of limestone due to contact metamorphism associated with magmatic intrusion into limestone. The magma cooled down and formed biotite-muscovite and granite. The reaction between country rock and the magmatic fluid introduced Fe-bearing impurities like magnetite and pyrrhotite into calcite [48].

In the case of P-4 sample, magnetite and pyrrhotite were found similar to the P-3 sample together with steel fragments/particles, which were introduced as a result of abrasion of grinding balls with each other and the steel liner of the ball mill [49, 50]. These results indicated that both Fe-bearing minerals inherent in the source rock and Fe-scrap from ball milling are the major impurities in this sample.

3.3. Effects of Magnetic Field Intensity and Feed Rate

To improve the quality of low-grade $CaCO_3$, the P-4 sample (i.e., underflow fraction of air classifier after ball mill) with the lowest $CaCO_3$ and highest Fe_2O_3 contents was used for magnetic separation experiments. Figure 3 shows the (a) yield percentage, (b) Fe_2O_3 content, and (c) $CaCO_3$ content of non-magnetic products after separation by IRMS at different magnetic field intensities (0.25, 0.35, and 0.45 T) and feed rates (2.4, 2.8, and 3.2 kg/h).

The results showed that most of the materials were recovered in the non-magnetic fraction. The yield percentage of non-magnetic products decreased when the magnetic field intensity increased but increased with higher feed rates (Fig. 3 (a)). This means that the lowest magnetic field intensity (i.e., 0.25 T) and highest feed rate (i.e., 3.2 kg/h) had the highest yield percentage at 84.1% while conditions whereby the highest magnetic field intensity (i.e., 0.45 T) and lowest feed rate (i.e., 2.4 kg/h) was used had the lowest yield percentage at 80.74%.

Figure 3 (b) showed that the Fe_2O_3 content of non-magnetic products were between 0.24% and 0.29%, which was lower than the original feed at 0.67%. The lowest Fe_2O_3 content was obtained at 0.45 T and 2.4 kg/h, indicating that high magnetic field intensity and low feed rate are required to produce low Fe_2O_3 content products.

In the case of $CaCO_3$ content, the range in the non-magnetic product was 98.3 to 98.6%, which was higher than that of the original feed at 98.1% (Fig. 3 (c)).

These results were in line with the previous studies that worked on the recovery of paramagnetic minerals (i.e., hematite [44] and low-grade ferruginous manganese ore [42]). The higher magnetic field intensity could recover/remove more magnetic materials due to more intensity of magnetization and magnetic force could occur and for feed rate, low feed rate could make each particle touch and be attached on the induced roll so, the magnetic particles have more chance to be recovered as magnetic products [17, 21, 42, 44].

These results suggest that when a magnetic field intensity of 0.45 T and feed rate of 2.4 kg/h was used, Fe-bearing impurities were effectively removed and acceptable $CaCO_3$ contents were achieved. However, the Fe_2O_3 content under these conditions still did not meet the standard required by the industry.

3.4. Effects of Cleaning by Repetitive Magnetic Separation

To achieve saleable quality of $CaCO_3$ products, the non-magnetic products were repeatedly fed into the IRMS to remove more magnetic materials and decrease their Fe_2O_3 content. Figure 4 illustrates the (a) yield percentage, (b) Fe_2O_3 content, and (c) $CaCO_3$ content of non-magnetic products after the separation using IRMS at magnetic field intensities of 0.45 T and feed rate of 2.4 kg/h with 1, 2, and 3 repetitions.

The yield percentage of non-magnetic products decreased when the samples were repeatedly treated by magnetic separation (Fig. 4 (a)). For the Fe_2O_3 content, the lowest amount was obtained after 3 repetitions (Fig. 4 (b)).

In the case of $CaCO_3$ content, the range in non-magnetic product was 98.3−98.6%, which was higher than that of the original feed (98.2%) (Fig. 4 (c)). These results showed that with 3 repetitions, the lowest Fe_2O_3 content with lowest yield and acceptable $CaCO_3$ content could be obtained, however, the content of Fe_2O_3 under these conditions still did not meet the standard required by the industry.

3.5. Optimization

From previous experiments, it was found that high magnetic field intensity and low feed rate are both required to achieve low Fe_2O_3 content products [13, 35]. However, the products obtained after magnetic separation still contain Fe_2O_3 exceeding the standard requirement of industries. In this section, optimization experiments were

DOI:10.4186/ej.2023.27.10.1

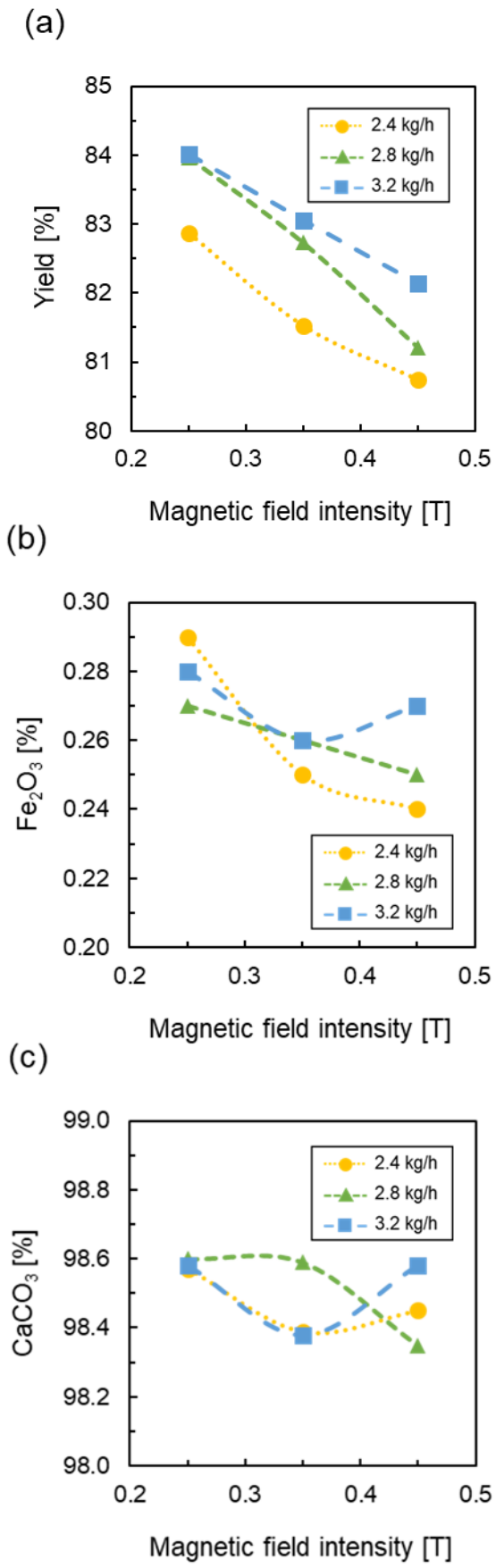

Fig. 3. (a) yield percentage, (b) Fe_2O_3 content, and (c) $CaCO_3$ content of non-magnetic products after magnetic separation experiments with different magnetic field intensities (0.25, 0.35, and 0.45 T) and feed rates (2.4, 2.8, and 3.2 kg/h).

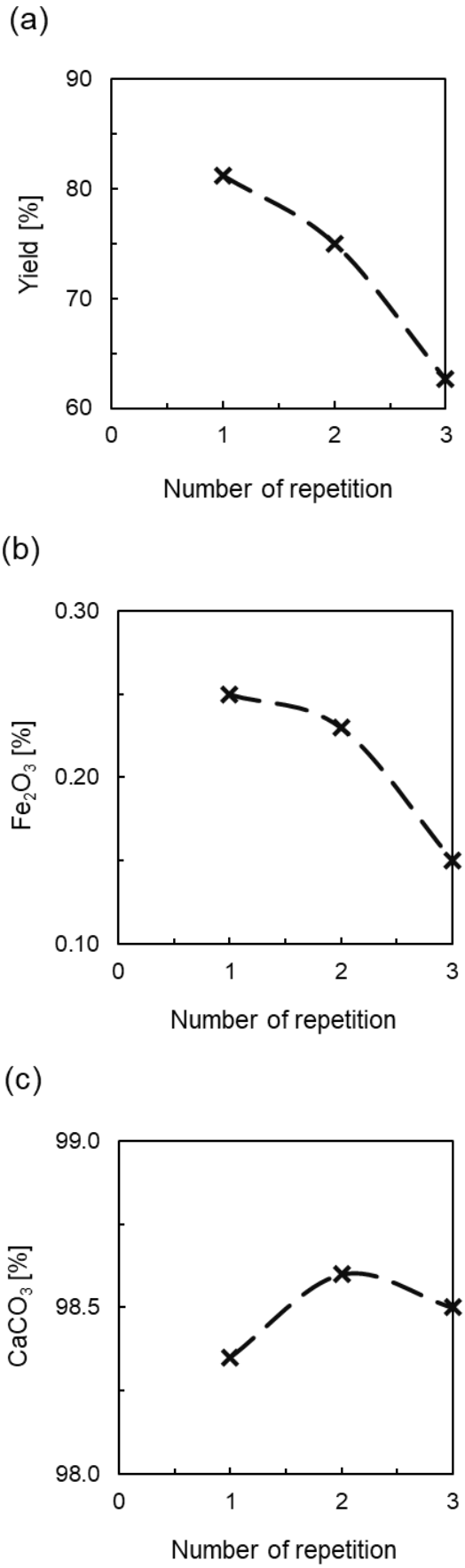

Fig. 4. (a) yield percentage, (b) Fe_2O_3 content, and (c) $CaCO_3$ content of non-magnetic products after magnetic separation experiments at 0.45 T and 2.4 kg/h with 1, 2, and 3 repetitions.

carried out using lower feed rates of 1.6, 2.0, and 2.4 kg/h with 4 repetitions and magnetic field intensity of 0.45 T (i.e., maximum magnetic field intensity of IRMS used in this study).

Similar to the previous experiments, the results showed that the yield percentage of non-magnetic products decreased with lower feed rates (Fig. 5 (a)). For the Fe_2O_3 content, it decreased at lower feed rates and the lowest Fe_2O_3 value of 0.08% was successfully obtained at 1.6 kg/h. and with this condition, the Fe_2O_3 content are acceptable for animal feeding ($Fe_2O_3 \leqslant 0.1\%$) (Fig. 5 (b)). For $CaCO_3$ content, the lower feed rates increased the $CaCO_3$ content up to 98.7% (Fig. 5 (c)).

These results indicate that low-grade $CaCO_3$ could be upgraded to acceptable quality using an IRMS with a magnetic field intensity of 0.45 T and feed rate of 1.6 kg/h after 4 repetitions.

4. Conclusions

In this study, a low-grade carbonate material collected from a processing plant in Thailand was characterized to identify the sources of Fe-bearing impurities and upgraded by magnetic separation (IRMS) to improve its quality. The results revealed that the Fe-bearing materials in the samples originated from the source rock and introduced by processing. Magnetite and pyrrhotite were identified as inherent gangue minerals in the source rock, which were formed due to contact metamorphism when biotite-muscovite and granite rocks intruded into the calcite-rich country rock. Meanwhile, synthetic Fe impurities originated from steel balls and liners used in ball milling.

To achieve the target quality of $CaCO_3$ for industrial applications, Fe_2O_3 content of the samples were removed by IRMS. The effects of magnetic field intensity, feed rate, and repetition on the yield percentage, Fe_2O_3 content, and $CaCO_3$ content were also evaluated. The results showed that low Fe_2O_3 with high content of $CaCO_3$ could be obtained at high magnetic field intensity, low feed rate, and repetitive IRMS treatment. Finally, an acceptable grade for animal feeding ($Fe_2O_3 \leqslant 0.1\%$) was successfully achieved when a magnetic field intensity of 0.45 T and feed rate of 1.6 kg/h were used after 4 repetitions.

Acknowledgement

The authors wish to thank the editor and reviewers for their valuable inputs to this paper.

References

[1] J. Rohleder and E. Kroker, *Calcium Carbonate: From the Cretaceous Period into the 21st Century*. Birkhäuser, 2012.

[2] F. W. Tegethoff, J. Rohleder, and E. Kroker, *Calcium Carbonate: From the Cretaceous Period into the 21st Century*. Springer Science & Business Media, 2001.

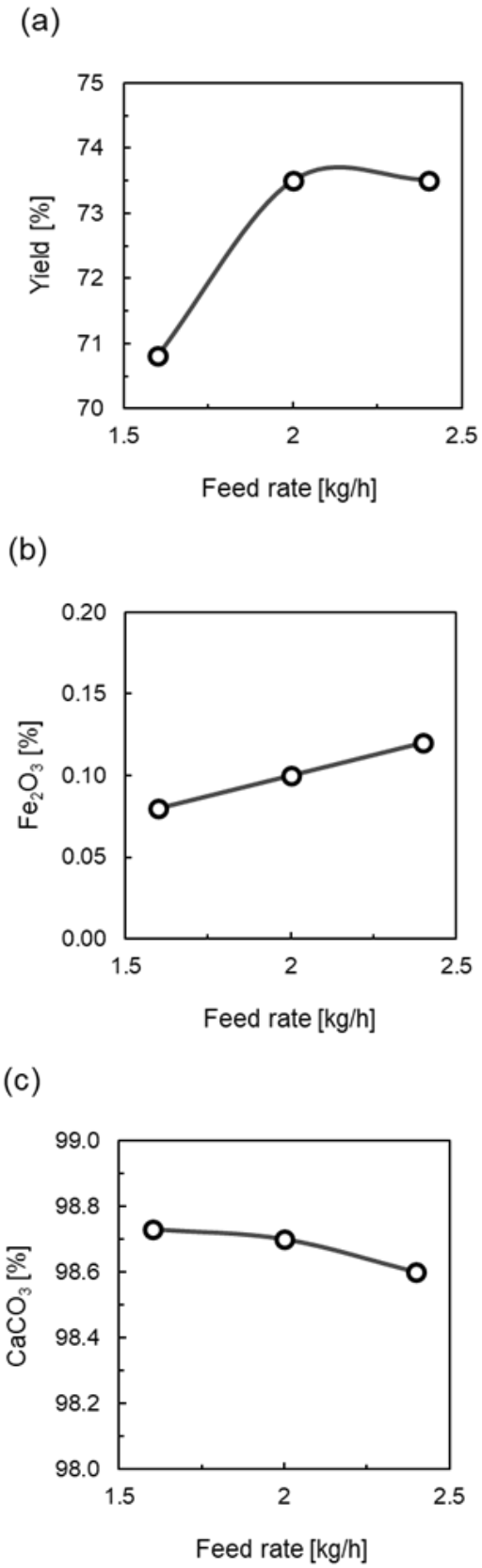

Fig. 5. (a) yield percentage, (b) Fe_2O_3 content, and (c) $CaCO_3$ content of non-magnetic products after magnetic separation experiments at 0.45 T and 4 repetitions with different feed rates (1.6, 2.0, and 2.4 kg/h).

[3] B. Wongkaewphothong, C. Kertbundit, P. Srichonphaisarn, P. Julapong, P. Homchuen, O. Juntarasakul, K. Maneeintr, C. B. Tabelin, A. Numprasanthai, S. Saisinchai, and T. Phengsaart, "The improvement in whiteness index of calcite tailings using attrition-scrubbing process," *Sep Sci Technol*, pp. 2077–2085, 2023.

[4] K. E. Eang, T. Igarashi, R. Fujinaga, M. Kondo, and C. B. Tabelin, "Groundwater monitoring of an open-pit limestone quarry: Water-rock interaction and mixing estimation within the rock layers by geochemical and statistical analysis," *Int J Min Sci Technol*, vol. 28, pp. 849–857, 2018.

[5] K. E. Eang, T. Igarashi, R. Fujinaga, M. Kondo, and C. B. Tabelin, "Groundwater monitoring of an open-pit limestone quarry: groundwater characteristics, evolution and their connections to rock slopes," *Environ Monit Assess*, pp. 190–193, 2018.

[6] C. B. Tabelin, T. Igarashi, M. Villacorte-Tabelin, I. Park, E. M. Opiso, M. Ito, N. Hiroyoshi, "Arsenic, selenium, boron, lead, cadmium, copper, and zinc in naturally contaminated rocks: A review of their sources, modes of enrichment, mechanisms of release, and mitigation strategies," *Sci Total Environ,* vol. 645, pp. 1522–1553, 2018.

[7] C. B. Cecil and C. F. Eble, "Paleoclimate controls on carboniferous sedimentation and cyclic stratigraphy in the appalachian basin," US Geological Survey, 1992.

[8] J. A. H. Oates, *Lime and Limestone: Chemistry and Technology, Production and Uses*. John Wiley and Sons, 2008.

[9] United Nations. "Transforming our world: the 2030 agenda for sustainable development." https://sustainabledevelopment.un.org/post2015/summit (accessed July 28, 2022).

[10] S. Owada, "A new trend of physical concentration in resources recycling," *Engineering Journal*, vol. 20, no. 4, pp. 12-136, 2016.

[11] D. Spelman and Y. Lee, "Sustainability of concrete as a civil engineering material," *Engineering Journal*, vol. 26, no. 7, pp. 69–81, 2022.

[12] S. Saisinchai, "Separation of PVC from PET/PVC mixtures using flotation by calcium lignosulfonate depressant," *Engineering Journal*, vol. 18, no. 1, pp. 45-54, 2013.

[13] E. Aghaei, Z. Wang, B. Tadesse, C. B. Tabelin, Z. Quadir, and R. D. Alorro, "Performance evaluation of Fe-Al bimetallic particles for the removal of potentially toxic elements from combined acid mine drainage-effluents from refractory gold ore processing," *Minerals.*, vol. 11, no. 6, p. 590, 2021.

[14] E. Aghaei, B. Tadesse, C. B. Tabelin, and R. D. Alorro, "Mercury sequestration from synthetic and real gold processing wastewaters using Fe-Al bimetallic particles," *J Clean Prod,* vol. 372, 2022.

[15] C. B. Tabelin, V. J. T. Resabal, I. Park, M. G. B. Villanueva, S. Choi, R. Ebio, P. J. Cabural, M. Villacorte-Tabelin, A. Orbecido, R. D. Alorro, S. Jeon, M. Ito, and N. Hiroyoshi, "Repurposing of aluminum scrap into magnetic Al0/ZVI bimetallic materials: two-stage mechanical-chemical synthesis and characterization of products," *J Clean Prod*, vol. 317, p. 128285, 2021.

[16] D. A. Norrgran and M. J. Mankosa, *SME Mining Engineers Handbook*. SME, 2006.

[17] S. K. Tripathy, P. K. Banerjee, N. Suresh, Y. R. Murthy, and V. Singh, "Dry high-intensity magnetic separation in mineral industry—A review of present status and future prospects," *Miner Process Extr Metall Rev*, vol. 38, no. 6, pp. 339–365, 2017.

[18] Z. Hu, J. Liu, L. Han, Y. Wang, D. Lu, X. Zheng, and Z. Xue, "Dynamic particle accumulation on a single wire in transverse field pulsating high gradient magnetic separator," *Miner Eng,* vol. 183, p. 107609, 2022.

[19] G. T. Mohanraj, S. Joladarashi, H. Hanumanthappa, B. K. Shanmugam, H Vardhan, G. M. Naik, P. D. Bhat, and M. R. Rahman, "Numerical approach for optimization of magnetic roller and evaluating the performance of permanent magnet roller separator through design of experiment," *Alex Eng J*, vol. 61, no. 12, pp. 13011–13033, 2022.

[20] Z. Yuan, X. Zhao, J. Lu, H. Lv, and L. Li, "Innovative pre-concentration technology for recovering ultrafine ilmenite using superconducting high gradient magnetic separator," *Int J Min Sci Technol,* vol. 31, no. 6, pp. 1043–1052, 2021.

[21] S. K. Tripathy, V. Singh, Y. R. Murthy, P. K. Banerjee, and N. Suresh, "Influence of process parameters of dry high intensity magnetic separators on separation of hematite," *Int J Miner Process,* vol. 160, pp. 16–31, 2017.

[22] F. Yi, L. Chen, J. Zeng, Y. Jiang, and X. Ren, "Separation characteristics of dry high-intensity drum magnetic separator," *Miner Eng,* vol. 189, p. 107861, 2022.

[23] Z. Hu, D. Lu, X. Zheng, Y. Wang, Z. Xue, and S. Xu, "Development of a high-gradient magnetic separator for enhancing selective separation: A review," *Powder Technol*, vol. 421, p. 118435, 2023.

[24] E. Charikinya, J. Robertson, A. Platts, M. Becker, P. Lamberg, and D. Bradshaw, "Integration of mineralogical attributes in evaluating sustainability indicators of a magnetic separator," *Miner Eng*, vol. 107, pp. 53–62, 2017.

[25] S. K. Tripathy, P. K. Banerjee, and N. Suresh, "Separation analysis of dry high intensity induced roll magnetic separator for concentration of hematite fines," *Powder Technol,* vol. 264, pp. 527–535, 2014.

[26] Z. Kheshti, K. A. Ghajar, R. Moreno-Atanasio, F. Neville, and S. Ghasemi, "Investigating the high gradient magnetic separator function for highly efficient adsorption of lead salt onto magnetic mesoporous silica microspheres and adsorbent recycling," *Chem Eng Process.: Process Intensif*, vol. 148, p. 107770, 2020.

[27] S. Zeng, W. Zeng, L. Ren, D. An, and H. Li, "Development of a high gradient permanent magnetic separator (HGPMS)," *Miner Eng*, vol. 71, pp. 21–26, 2015.

[28] S. K. Baik, D. W. Ha, J. M. Kwon, Y. J. Lee, and R. K. Ko, "Magnetic force on a magnetic particle within a high gradient magnetic separator," *Physica C Supercond*, vol. 484, pp. 333–337, 2013.

[29] S. Nedelcu and J.H.P. Watson, "Magnetic separator with transversally magnetised disk permanent magnets," *Miner Eng*, vol. 15, no. 5, pp. 355–359, 2002.

[30] P. Todd, R. P. Cooper, J. F. Doyle, S. Dunn, J. Vellinger, and M. S. Deuser, "Multistage magnetic particle separator," *J Magn Magn Mater*, vol. 225, no. 1–2, pp. 294–300 , 2001.

[31] P. A. Augusto, T. Castelo-Grande, P. Augusto, D. Barbosa, and A.M. Estévez, "Supporting theory of a new magnetic separator and classifier. Equations and modeling: Part II – Magnetic particles," *Curr Appl Phys*, vol. 7, no. 3, pp. 247–257 , 2007.

[32] Z. Kheshti, K. A. Ghajar, A. Altaee, and M. R. Kheshti, "High-Gradient Magnetic Separator (HGMS) combined with adsorption for nitrate removal from aqueous solution," *Sep Purif Technol*, vol. 212, pp. 650–659, 2019.

[33] E. A. Mendrela and E. M. Mendrela, "Magnetic separator for chimney dust," *J Magn Magn Mater*, vol. 94, no. 1–2, pp. 191–193, 1991.

[34] J. Svoboda and V. E. Ross, "Particle capture in the matrix of a magnetic separator," *Int J Miner Process*, vol. 27, no. 1–2, pp. 75–94, 1989.

[35] C. Wang, J. Qian, K. Wang, X. Yang, Q. Liu, N. Hao, C. Wang, X. Dong, and X. Huang, "Colorimetric aptasensing of ochratoxin A using Au@Fe_3O_4 nanoparticles as signal indicator and magnetic separator," *Biosens Bioelectron*, vol. 77, pp. 1183–1191, 2016.

[36] C. Bin, Y. Yi, S. Zhicheng, W. Qiang, A. Abdelkader, A. R. Kamali, and D. Montalvão, "Effects of particle size on the separation efficiency in a rotary-drum eddy current separator," *Powder Technol,* vol. 410, p. 117870, 2022.

[37] N. Soonthornwiphat, S. Saisinchai, and P. Parinayok, "Recovery slime waste from feldspar flotation plant at Attanee International Co. Ltd., Tak Province, Thailand," *Engineering Journal*, vol. 20, no. 4, pp. 69–78, 2016.

[38] S. Saisinchai, T. Boonpramote, and P. Meechumna, "Upgrading feldspar by WHIMS and flotation techniques," *Engineering Journal*, vol. 19, no. 4, pp. 83–92, 2015.

[39] S. Saisinchai, T. Boonpramote, and P. Meechumna, "Recovery of fine cassiterite from tailing dump in Jarin Tin Mine, Thailand," *Eng J*, vol. 20, no. 4, pp. 41–49, 2016.

[40] S. S. Ibrahim, M. M. Farahat, and T. R. Boulos, "Optimizing the performance of the RER magnetic separator for upgrading silica sands," *Part Sci Technol*, vol. 35, no. 1, pp. 21–28, 2015.

[41] P. K. Naik, "Quantification of induced roll magnetic separation of mineral sands," *Scand J Metal*, vol. 31, no. 6, pp. 367–373. 2002.

[42] V. Singh, T. K. Ghosh, Y. Ramamurthy, and V. Tathavadkar, "Beneficiation and agglomeration process to utilize low-grade ferruginous manganese ore fines," *Int J Miner Process*, vol. 99, 1–4, pp. 84–86. 2011.

[43] S. K. Tripathy, P. K. Banerjee, and N. Suresh, "Separation analysis of dry high intensity induced Roll Magnetic separator for concentration of hematite 52 fines," *Powder Technol, vol.* 264, pp. 527–535, 2014.

[44] S. K. Tripathy and N. Suresh, "Influence of particle size on dry high-intensity magnetic separation of paramagnetic mineral," *Adv Powder Technol*, vol. 28, no. 3, pp. 1092–1102. 2017.

[45] E. M. Opiso, C. B. Tabelin, C. V. Maestre, J. P. J. Aseniero, I. Park, and M. Villacorte-Tabelin, "Synthesis and characterization of coal fly ash and palm oil fuel ash modified artisanal and small-scale gold mine (ASGM) tailings based geopolymer using sugar mill lime sludge as Ca-based activator," *Heliyon*, vol. 7, no. 4, p. e06654, 2021.

[46] T. Tatsuhara, T. Arima, T. Igarashi, and C. B. Tabelin, "Combined neutralization-adsorption system for the disposal of hydrothermally altered excavated rock producing acidic leachate with hazardous elements," *Eng Geol.* vol. 139–140, pp. 76–84, 2012.

[47] S. Tamoto, C. B. Tabelin, T. Igarashi, M. Ito, and N. Hiroyoshi, "Short and long term release mechanisms of arsenic, selenium and boron from a tunnel-excavated sedimentary rock under in situ conditions," *J Contam Hydrol*, vol. 175–176, pp. 60–71, 2015.

[48] C. Tantisukrit, "Review of the metallic mineral deposits of Thailand," *3rd Region Conference Geology Mineral Resources of Southeast Asia*, Bangkok, Thailand, 1978, pp. 783–793.

[49] F. Moosakazemi, M. R. T. Mohammadi, M. Mohseni, M. Karamoozian, and M. Zakeri, "Effect of design and operational parameters on particle morphology in ball mills," *Int J Miner Process*, vol. 165, pp. 41–49, 2017.

[50] A. Sato, J. Kano, and F. Saito, "Analysis of abrasion mechanism of grinding media in a planetary mill with DEM simulation," *Adv Powder Technol*, vol. 21, no. 2, pp. 212–216, 2010.

Pimpichcha Teawpanich, photograph and biography not available at the time of publication.

Somsak Saisinchai, photograph and biography not available at the time of publication.

Apisit Numprasanthai, photograph and biography not available at the time of publication.

Raphael Bissen, photograph and biography not available at the time of publication.

Onchanok Juntarasakul, photograph and biography not available at the time of publication.

Carlito Baltazar Tabelin, photograph and biography not available at the time of publication.

Theerayut Phengsaart, photograph and biography not available at the time of publication.